

HARU: Haptic Augmented Reality-Assisted User-Centric Industrial Network Planning

Qi Liao*, Nikolaj Marchenko†, Tianlun Hu*, Peter Kulics*, Lutz Ewe*

*Nokia Bell Labs, Stuttgart, Germany

†Corporate Research and Advanced Engineering, Robert Bosch GmbH, Renningen, Germany

E-Mails: {qi.liao, peter.kulics, lutz.ewe}@nokia-bell-labs.com,

Nikolaj.Marchenko@de.bosch.com, tianlun.hu@nokia.com

Abstract—To support Industry 4.0 applications with haptics and human-machine interaction, the sixth generation (6G) requires a new framework that is fully autonomous, visual, and interactive. In this paper, we provide an end-to-end solution, HARU, for private network planning services, especially industrial networks. The solution consists of the following functions: collecting visual and sensory data from the user device, reconstructing 3D radio propagation environment and conducting network planning on a server, and visualizing network performance with augmented reality (AR) on the user device with enabled haptic feedback. The functions are empowered by three key technical components: 1) vision- and sensor fusion-based 3D environment reconstruction, 2) ray tracing-based radio map generation and network planning, and 3) AR-assisted network visualization enabled by real-time camera relocalization. We conducted the proof-of-concept in a Bosch plant in Germany and showed good network coverage of the optimized antenna location, as well as high accuracy in both environment reconstruction and camera relocalization. We also achieved real-time AR-supported network monitoring with an end-to-end latency of about 32 ms per frame.

I. INTRODUCTION

Impacted by the ever-increasing global spending on smart manufacturing, the total addressable market for private networks is forecast to increase from \$3.7 billion in 2021 to over \$109.4 billion in 2030, according to a report by ABI Research [1]. However, the state-of-the-art network planning services remain old-fashioned. For example, the network planning service providers rely on either user-uploaded floor plan or on-site measured site survey. Not only are such services costly in both time and human resources, but they also provide a limited user experience. Moreover, the modern flexible and modular production systems require industrial network planning solutions to be quickly adapted to new network environments triggered by dynamically changing batches of individual products.

Extended reality and digital twin can be promising technologies to facilitate autonomous and interactive network services in the 6G era [2], [3]. However, most of the works provided perspective on the challenges they raise to future network systems, e.g., as emerging 5G use cases [4], while few of the works considered them as a means to help build truly user-centric, interactive cyber-physical network systems [5]. A few works proposed conceptual AR-based frameworks for various small-scale network solutions. For example, WiART [6] takes inputs from beam-steerable reconfigurable antennas and enables users to select desired antenna radiation patterns in the mobile app and observe their effects on link performance. However, the AR visualization is limited to the antennas and their radiation patterns within a short distance. In [5], the authors proposed to scan an indoor apartment environment to

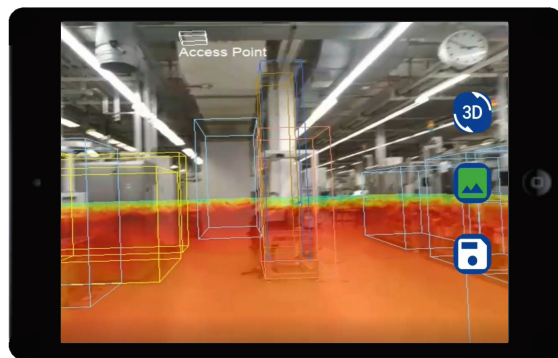


Fig. 1: Haptic AR-assisted network planning app

a vector facet model and use it for wireless signal propagation prediction with ray tracing. Then, an AR application is applied to visualize the prediction in the form of holograms with an AR headset. However, the performance is limited by the lack of information about the obstacles for radio propagation. Also, the solution requires licensed AR applications and expensive commercial AR headsets. To provide autonomous, visual, and interactive service for private network planning with low-cost mobile devices, in [7] and [8], we proposed HARU, a haptic augmented reality-assisted user-centric network planning solution, enabled by *vision- and sensor fusion-based 3D radio environment reconstruction* and *AR-assisted network visualization*. The goal is to make the invisible radio network visible and provide truly user-centric, gamified, haptic interface to improve user experience. The service platform receives video/image sequence and inertial measurement unit (IMU) data from the user device via a mobile user interface (UI), reconstructs the 3D radio environment based on the received data, approximates the radio propagation model, and demonstrates the optimized network planning solution based on the user's haptic feedback on UI with AR, as shown in Fig. 1. A prerequisite for enabling AR is to estimate *6D camera pose* (including 3D position and 3D orientation) in real time, known as the *camera relocalization* problem. With the estimated camera pose, we can project the virtual objects from the real-world coordinate system back to the camera coordinate system. In our previous works [9], [10], we have provided technical solutions and algorithms for individual functions, *3D radio environment reconstruction* and *real-time camera relocalization*, respectively. In this paper, we focus on the system design of the end-to-end solution and its application to a real industrial environment. Note that in the previous works, we conducted the experiments in a small-scale office environment only, while in this paper we demonstrate the most recent results of the proof-of-concept (PoC) in a Bosch

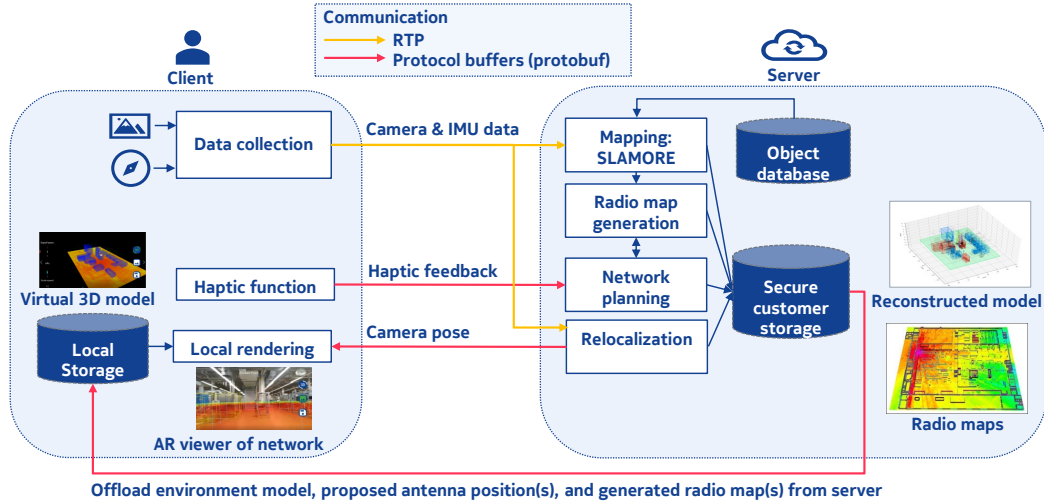


Fig. 2: Architecture of the end-to-end AR-empowered network planning solution

plant in Germany. To the best of the authors’ knowledge, we provide the first end-to-end interactive AR-assisted solution to industrial network planning. Our contributions are summarized as follows.

- On the client side, we developed an Android app, which sends visual and sensory data from the mobile device to a server, receives model and localization data from the server, and performs local rendering and haptic function for the interactive interface.
- On the server side, we developed and implemented the following functions: 1) a **3D environment reconstruction** algorithm called simultaneous localization and mapping with object recognition (SLAMORE) [9], which can detect, track, localize, and reconstruct the major obstacles for electromagnetic waves, 2) a **network planning policy** assisted by ray-tracing application, and 3) a **real-time camera relocalization** algorithm [10] based on deep learning and sensor fusion to enable the AR features.
- We demonstrated the PoC of the end-to-end solution with a standard Android mobile device and the edge server in the **real industrial environment** – a Bosch plant in Germany, and achieved an end-to-end delay (including data compression, communication, and computation) of about 32 ms per frame.

II. SYSTEM ARCHITECTURE

The proposed haptic AR-assisted network planning service platform includes three main techniques: 1) mapping and 3D industrial environment reconstruction, 2) ray tracing-based radio map generation and network planning, and 3) real-time camera relocalization for AR features. Because the remote service aims to provide real-time AR experience for monitoring and interacting with the network, we need to allocate the different functions in either the mobile device or the server based on their computational, transmission, and latency constraints. After extensive experiments, we design the system architecture of the end-to-end solution as shown in Fig. 2. We decide to load the reconstructed 3D model and radio maps from the server to the device, such that the AR rendering function can be called locally. In general, local rendering function responds much faster to user’s inputs for interaction, compared to remote

rendering. Moreover, because our SLAMORE algorithm only extracts and reconstructs objects relevant to radio propagation, the size of data is small (less than 5 MB) to be transferred and locally stored. On the other hand, camera relocalization is performed on the server because the deep learning-based model is relatively large and real-time local inference is computationally inefficient.

In the first step (**mapping**), the user runs our app on a mobile device and the app sends the captured visual and sensory data to the server. The server receives the data and calls the mapping function – our developed SLAMORE algorithm [9] – to detect, track, localize, and reconstruct the major obstacles for electromagnetic waves. In this way, the server reconstructs an “extracted” version of the environment customized for radio propagation. Such a sparse reconstruction of the environment significantly eases the computation of ray tracing for further steps of radio map generation and network planning.

In the second step (**interactive network planning**), with the haptic function, the user can specify a preferred area (e.g., where a power supply is available) for access point (AP) deployment and send the information to the server. The server generates radio maps with ray tracing based on the reconstructed 3D environment, and performs network planning policy constrained by the user-specified area. Then, the server sends the extracted environment model, the proposed AP deployment position(s), and the corresponding generated radio map(s) to the user. The data is saved in the local storage and can be retrieved locally to enable haptic interaction with the virtual 3D model of the network environment.

In the final step (**AR-assisted network monitoring**), the server trains a multi-input deep neural network (DNN) for camera relocalization [10], based on the previously collected data and the generated environment in the mapping step. The user sends the visual and sensory data to the server in real time, and the relocalization model takes it as input and estimates the 6D camera pose as output. The server then sends the estimated camera pose to the user device, and the app computes rendering locally and projects the augmented radio map on the captured camera view.

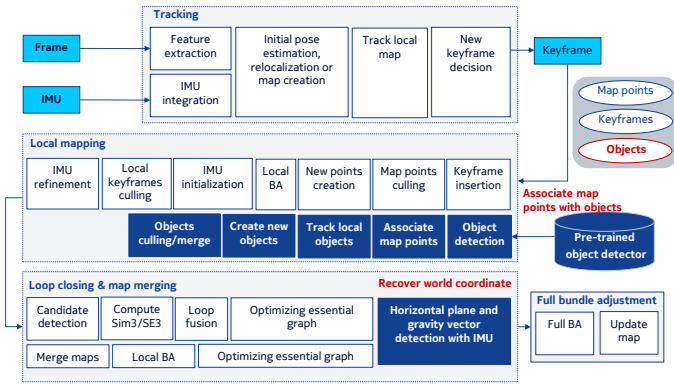


Fig. 3: SLAMORE architecture, where Sim3/SE3 stands for 3D affine transform and BA means the bundle adjustment. The white blocks are the original functions from ORB-SLAM3 [11], while the blue blocks are our developed and embedded functions for 3D object reconstruction and plane detection.

III. END-TO-END SOLUTION

In this section, we describe the following technical components of the end-to-end solution: 1) data collection and preprocessing, 2) mapping and 3D radio environment reconstruction, 3) 3D radio map generation and network planning, and 4) real-time camera relocalization.

A. Data Collection and Preprocessing

The app running on mobile device captures in real time the RGB camera stream and the motion sensor measurements, including *timestamp*, *3D angular rate*, *3D linear acceleration*, and *4D quaternion* from the device, and sends them to the server via real-time transport protocol (RTP) (details of the implementation will be given in Section IV-1). These measurements are used for both 3D environment reconstruction and camera relocalization algorithms.

On the server, to facilitate SLAMORE and reconstruct an obstacle-aware radio propagation environment, a labelled dataset of finite objects in the industrial environment needs to be pre-collected. One may argue that in practice the pretrained set of object classes can be too large for recognizing all obstacles in the new environments. However, because we target private networks, we can train multiple sets of classes for different types of customers. For example, automotive manufacturing plants from various manufacturers possibly have deployed similar types of equipment, thus we can create a large dataset for this specific type of customers.

B. Mapping and 3D Radio Environment Reconstruction

Most of the mapping and environment reconstruction methods, such as 3D scanning or simultaneous localization and mapping (SLAM) algorithms, provide complex reconstructed models by creating ultra-dense 3D point cloud (a collection of points defined by a given coordinate system) and recovering smooth nonlinear surfaces [12]. However, for radio propagation environment reconstruction we cannot afford such complexity: modeling radio propagation maps, e.g., by using ray tracing [13], can be computationally extremely expensive if it is based on a complex environment. Thus, to customize an environment reconstructor for 3D radio propagation modeling, we target the following problem:

How to efficiently reconstruct an “extracted” industrial radio propagation environment that achieves good accuracy yet eases the task of 3D radio propagation modeling?

To this end, we propose a feature- and object-based monocular SLAM algorithm called SLAMORE [9], which can efficiently detect, track, localize, and reconstruct the major obstacles for electromagnetic waves. It extracts the industrial network environment composed of reconstructed obstacles for radio propagation and detected space boundaries. SLAMORE is built on the basis of a state-of-the-art visual-inertial SLAM algorithm ORB-SLAM3 [11]. However, ORB-SLAM3 reconstructs the environment with sparse 3D point cloud and the output point cloud does not provide the information needed for radio propagation modeling, such as real-world coordinates and scale, object segmentation, and surface material. To overcome this challenge, we propose SLAMORE with the following new features, as shown in Fig. 3: 1) We train a *customized convolutional object detector* for a defined set of objects in industrial radio propagation environment. The label includes the class of the object, 3D shape and size, and surface material. 2) A series of new functions are embedded in the local mapping thread for 3D object reconstruction and called for every keyframe, including *object detection*, *associating map points to objects*, *object tracking*, *new object creation*, and *object culling and merging*. 3) We solve the major problem in ORB-SLAM3 when using low-cost and low-frequency IMU sensors from mobile device – *recovery of the real-world coordinates and scale* – by using the side information contained in the class labels of the recognized objects and by filtering the IMU measurements.

With these new features, we can extract sufficient but not overwhelming information about the environment, to be further used as the input for the efficient radio propagation modeling. Due to the limited space, we refer the interested readers to our previous work [9] for the technical details.

C. 3D Radio Map Generation and Network Planning

Because ray tracing for radio propagation modeling is a well-studied topic, we can use existing algorithms or software development kits (SDKs) to compute the radio map such as WinProp [14] and WISE [15]. Also, to further reduce complexity, various shooting-and-bouncing ray tracing algorithms [16] can be applied. Moreover, because SLAMORE is customized for reconstructing radio propagation environment, it allows more efficient computation of ray tracing, comparing to the complex 3D scan composed of huge nonlinear triangular meshes. With ray tracing, we can obtain the reference signal received power (RSRP) values of any point in the 3D space. For efficient network planning, we can discretize the bounded 3D space $\mathcal{S} := [x^{(\min)}, x^{(\max)}] \times [y^{(\min)}, y^{(\max)}] \times [z^{(\min)}, z^{(\max)}]$ into equally-spaced nonoverlapping voxels. Thus, the 3D RSRP map can be computed for each antenna position $\mathbf{a} \in \mathcal{S}$, denoted by $\mathbf{P}(\mathbf{a}) := [p_{i,j,k}(\mathbf{a})]$, where $p_{i,j,k}(\mathbf{a})$ denotes the RSRP at the voxel with indices (i, j, k) in x, y, z dimensions, respectively.

The network planning aims to provide good coverage of the factory by optimizing the position of AP $\mathbf{a} \in \mathcal{S}$, especially where the machines/devices equipped with transceivers are located. We define the utility function as the weighted sum of RSRP over all voxels, while assigning higher weights to the

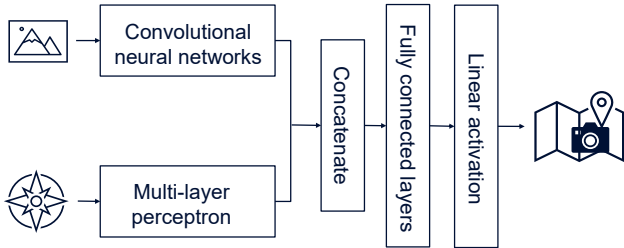


Fig. 4: Multi-input DNN for real-time camera relocalization

following types of voxels: 1) those associated to the machine objects which generate network traffic, and 2) those associated to the defined trajectory of mobile objects such as automated guided vehicles (AGVs). The optimization problem is then defined as

$$\max_{\mathbf{a} \in \mathcal{S}} U(\mathbf{a}), \text{ s.t. } U(\mathbf{a}) = \sum_{i,j,k} w_{i,j,k} p_{i,j,k}(\mathbf{a}). \quad (1)$$

Because of the interactive interface and the haptic functions, the users can specify their preferred deployment areas, e.g., a limited area on the ceiling, denoted by \mathcal{S}' . Thus, the searching space \mathcal{S} is further reduced to \mathcal{S}' and we can replace \mathcal{S} with \mathcal{S}' in (1). We consider the gradient-based search over \mathcal{S}' . For efficient searching, we define the initial point as the geometric center \mathbf{c} of all detected machines/devices. Then, we generate N searching instances, each starts from a distinct initial position sampled near \mathbf{c} . We perform gradient-based search for each of the instances, and choose the one with the maximum converged utility among all instances. Note that the gradient-based search is an iterative process, i.e., we need to compute the radio map for each iterative AP position, thus a fast yet accurate ray tracing computation is crucial to reduce the complexity. SLAMORE well fulfills the task, because it extracts sufficient but not overwhelming information about the environment, which further enables faster ray tracing computation.

D. Real-Time Camera Relocalization to Enable AR

To enable the AR features, e.g., overlaying the virtual radio map on the 2D images captured by camera, we need to estimate the 6 degrees of freedom (DoF) camera pose $\mathbf{p} := [\mathbf{l}, \mathbf{o}]$ consisting of camera location \mathbf{l} and orientation \mathbf{o} in real time. Therefore, we are interested in solving the following problem:

At each time frame t , given camera captured image array $\mathbf{I}(t) \in \mathbb{R}^{w \times h \times 3}$, where w and h are the image width and height in pixel respectively, and the extracted feature vector from motion sensors $\mathbf{m}(t) \in \mathbb{R}^n$, what is the corresponding camera pose $\mathbf{p}(t) := [\mathbf{l}(t), \mathbf{o}(t)]$ composed of camera location $\mathbf{l} := [x, y, z]$ and orientation \mathbf{o} ?

Note that the orientation \mathbf{o} can be written in the form of 3D rotation vector $\mathbf{r} := [r_x, r_y, r_z]$ or its equivalent 4D quaternion $\mathbf{q} := [q_x, q_y, q_z, q_w]$. The quaternion \mathbf{q} needs to be normalized to unit length, thus the camera pose is still 6-DoF when $\mathbf{o} = \mathbf{q}$.

To solve the problem, we propose a multi-input DNN including both image and sensor data in the inputs. The architecture of the DNN is shown in Fig. 4. The input image is resized to $(224, 224, 3)$ and fed into a pretrained convolutional neural network (CNN) backbone for object detection, such as MobileNetV2 [17]. To accelerate the learning, we load the

weights of the pretrained CNN object detector for SLAMORE as initial weights, since it is customized for the predefined object classes in the interested industrial environment. The sensor input is then passed through a multi-layer perceptron (MLP) composed of three dense (fully connected) layers with ReLU activation. The output layers of the CNN and MLP are concatenated and followed with 5 more dense layers with ReLU activation. Finally, the output layer with linear activation provides the camera pose estimation. The training data can be obtained from the data previously collected for SLAMORE, including the video sequence, the IMU data, and the corresponding camera pose in the world coordinate system. Due to the limited space, we omit the details here but refer the interested readers to our previous work [10].

After deriving the estimated camera pose in the world coordinate system, denoted by location $\mathbf{l}_w \in \mathbb{R}^3$ and rotation $\mathbf{R}_{cw} \in \mathbb{R}^{3 \times 3}$ (rotation matrix from the camera coordinate system to the world coordinate system, converted from orientation \mathbf{o}), we can project any 3D point of radio map \mathbf{p}_w in the world coordinate system into the pixel system (u, v) as below:

$$\begin{bmatrix} u' \\ v' \\ \alpha \end{bmatrix} = \mathbf{K} \mathbf{R}_{cw}^T [\mathbf{p}_w - \mathbf{l}_w], \quad (2)$$

$$u = u'/\alpha \text{ and } v = v'/\alpha, \quad (3)$$

where $\mathbf{R}_{cw}^T = \mathbf{R}_{wc}$ indicates the rotation matrix from the world to the camera coordinate system, $\mathbf{K} \in \mathbb{R}^{3 \times 3}$ is the camera intrinsic matrix, and $\alpha \neq 0$ is the scaling factor learned by SLAMORE.

IV. PROOF-OF-CONCEPT

We conducted the experiment in a Bosch plant in Germany, and selected an area of $15\text{m} \times 10\text{m}$. The applied antenna model is Nokia FW2HC integrated omni antenna with antenna gain of 4.7 dBi. We use Nokia 6 as the mobile device and the edge server is equipped with 4 Nvidia Tesla K80 GPUs for SLAMORE and DNN training and inference.

1) Data Collection and Communication Protocols

Our developed Android app captures RGB camera stream with a resolution of 480p and the motion sensor measurements including *timestamp*, *3D angular rate*, *3D linear acceleration* (from accelerometer), and *4D quaternion* (from Android attitude composite sensors which derive the rotation vector from the physical sensors accelerometer, gyroscope, and magnetometer). Note that many mobile devices are equipped with low-cost magnetometers and the reported quaternion can be very noisy. A low-pass filter is applied to the sensor output to reduce noise artifacts and smooth the signal reading. We use RTP to carry the video stream compressed by codec. The sensory data is also included in the RTP packets along with the video stream since the RTP specification allows for a custom extension to the protocol.

2) 3D Radio Environment Reconstruction

To test SLAMORE, we collected 5 video sequences, which provided 80596 frames in total. For training the object detector, we manually labelled only 300 keyframes with 25 classes of machines and objects in the industrial environment. The object detector is initialized with the SSD MobileNetV2 [17]

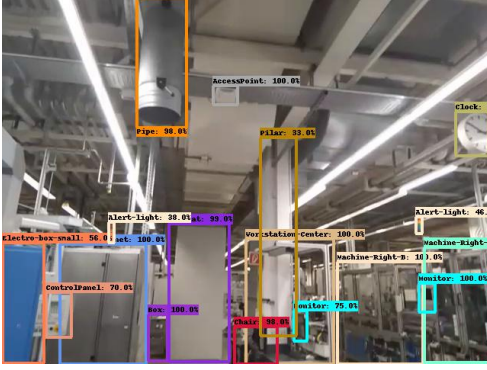


Fig. 5: Object detection customized to industrial environment

backbone model from Tensorflow 2 Object Detection API and finetuned with our labelled data collected from the industrial environment. Although the number of labelled training data is limited, we are able to achieve 87.2% mean average precision. An example of the detected objects in a frame is given in Fig. 5.

Then, for every keyframe, we project the detected map points in the 3D space back into the 2D camera view and adaptively associate them to the bounding boxes detected by the object detector. By clustering the 3D map points associated to the objects, and, with the shape information contained in the object’s label, we can estimate the position of the objects. We evaluate the performance with the average object-based root mean square error (RMSE) defined as $(1/K) \cdot \sum_{k=1}^K \sqrt{\sum_{i \in \{x,y,z\}} (p_i - \hat{p}_i)^2 / 3}$, where K is the number of detected objects, p_i and \hat{p}_i are the ground-truth and the estimated object’s position in $i \in \{x, y, z\}$ axis. We achieve the averaged RMSE of 0.2564 m over all detected objects within the selected area of $15\text{m} \times 10\text{m}$.

In Fig. 6 we compare the output of our proposed SLAMORE with the state-of-the-art output of the mapping computed from ORB-SLAM3 [11]. On the left side of the figure we show the raw outputs of ORB-SLAM3, including the map points as the black points and the estimated camera positions as the red trajectory, with inaccurate alignment with the world coordinates and without object segmentation. The poor alignment is caused by the noisy measurements from the low-cost IMU sensors in the mobile device. On the right side we show the output of SLAMORE, providing the reconstructed environment and obstacles for radio propagation environment, and the map points associated to distinct obstacles.

3) 3D Radio Map Generalization and Network Planning

In this experiment, we call the functions from WinProp [14] to compute the radio map with ray tracing technique. The heuristic searching algorithm described in Section III-C converges between 20 and 40 steps for each randomly initialized instance, which, in total costs less than 1 hour to perform the network planning task for the 3D industrial space. The generated radio maps of the optimized antenna position at different heights 10 cm, 100 cm, and 150 cm are shown in Fig. 7. In Fig. 8 we show that the optimized antenna position significantly improves the coverage at all three heights.

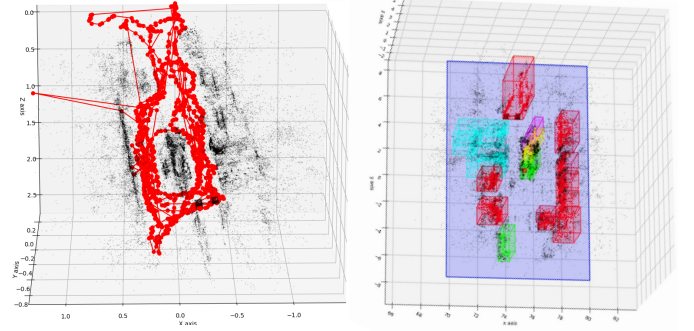


Fig. 6: [Left] Unaligned coordinates with detected map points with ORB-SLAM3. [Right] Reconstructed environment with the recognized 3D obstacles using SLAMORE.

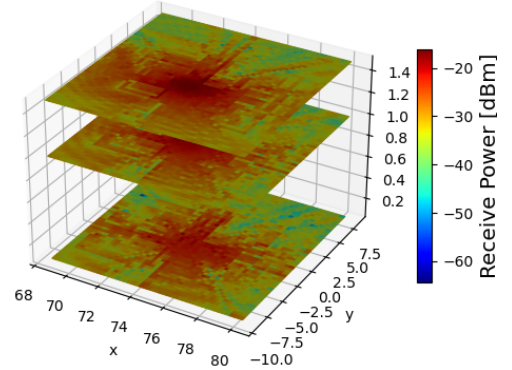


Fig. 7: Generated radio map of the optimized AP position

4) Real-Time Camera Relocalization

Either rotation vector (radians) $\mathbf{r} \in \mathbb{R}^3$ or quaternion $\mathbf{q} \in \mathbb{R}^4$ can be used to represent the camera orientation. In Table I we compare the output features \mathbf{r} and \mathbf{q} when using different loss functions: 1) **W_Euc_Euc**: weighted sum of location Euclidean distance and quaternion Euclidean distance, and 2) **W_Euc_Ang**: weighted sum of location Euclidean distance and quaternion angle error. Table I shows that using quaternion \mathbf{q} as output and including angle error in the loss function provides the best performance. The average inference time per frame is 3.87 ms.

TABLE I: Comparison of loss function and output features

	$\mathbf{o} = \mathbf{r}$ W_Euc_Euc	$\mathbf{o} = \mathbf{q}$ W_Euc_Euc	$\mathbf{o} = \mathbf{q}$ W_Euc_Ang
Mean location error	9.2124 cm	10.3212 cm	8.2937 cm
Mean orientation error	8.8237°	5.6327°	3.5262°

5) Performance of the End-to-End Solution

For the AR-empowered network visualization, we achieve the end-to-end latency (including data processing, data transmission, control message transmission, and deep learning-based model inference) of 31.83 ms per frame, i.e., frame rate of over 30 fps. We can also interact with the virtual 3D model as shown in Fig. 9a or monitor the network with an AR view in real time as shown in Fig. 9b.

V. CONCLUSION AND FUTURE WORK

We proposed a novel, interactive, and AR-assisted framework for industrial network planning service. We provided an

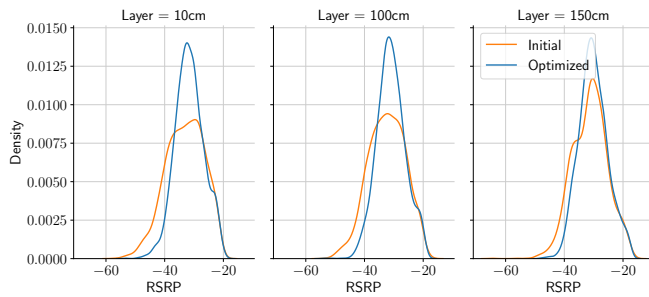
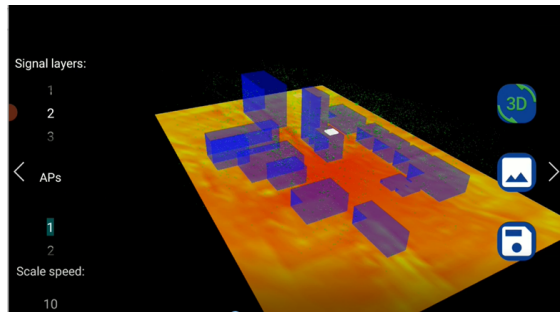
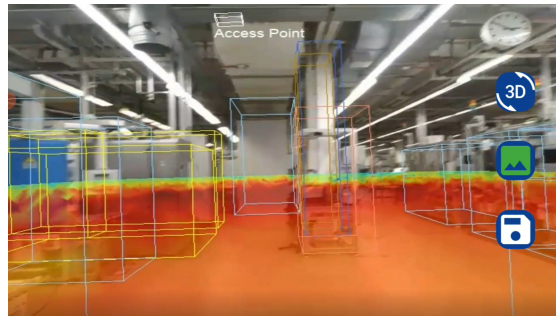


Fig. 8: Comparison of the RSRP distribution between initial and optimized antenna positions at different heights.



(a) Interactive birdview of the reconstructed 3D virtual network. User can choose different height layers and antenna positions to switch the view of the network.



(b) Real-time AR-assisted network monitoring, with augmented radio propagation map and detected objects.

Fig. 9: Developed UI of the Android app

end-to-end solution, which receives visual and sensory data from the mobile device, reconstructs the 3D industrial network environment, performs network planning in the server, and visualizes the network with AR on the mobile device. Several building blocks were developed: 1) SLAMORE algorithm to reconstruct the customized radio propagation environment for the factory, 2) ray tracing-based radio map generation and network planning, and 3) deep learning- and sensor fusion-based real-time camera relocation to enable the AR features. Finally, we conducted the PoC of the proposed end-to-end solution in a Bosch factory in Germany and showed good coverage of the optimized antenna location, as well as high accuracy in both environment reconstruction and camera relocation. We also achieved the real-time end-to-end latency of less than 32 ms per frame for the AR-empowered network monitoring. The future work includes further scaling up and accelerating the algorithms for larger factory space.

ACKNOWLEDGMENT

This work was supported by the German Federal Ministry of Education and Research (BMBF) project KICK [16KIS1102K]. We thank Csaba Szabo for his contribution to this project. Partial contents of this paper appear in [9] and [10].

REFERENCES

- [1] ABI Research, "The role of 5G in ICT transformation," Feb. 2022.
- [2] H. Viswanathan and P. E. Mogensen, "Communications in the 6G era," *IEEE Access*, vol. 8, pp. 57 063–57 074, 2020.
- [3] H. X. Nguyen, R. Trestian, D. To, and M. Tatipamula, "Digital twin for 5G and beyond," *IEEE Communications Magazine*, vol. 59, no. 2, pp. 10–15, 2021.
- [4] H. H. H. Mahmoud, A. A. Amer, and T. Ismail, "6G: A comprehensive survey on technologies, applications, challenges, and research problems," *Transactions on Emerging Telecommunications Technologies*, vol. 32, no. 4, p. e4233, 2021.
- [5] G. Koutitas, V. Kumar Siddharaju, and V. Metsis, "In Situ wireless channel visualization using augmented reality and ray tracing," *Sensors*, vol. 20, no. 3, p. 690, 2020.
- [6] D. H. Nguyen, J. Chacko, L. Henderson, A. Paatelma, H. Saarnisaari, N. Kandasamy, and K. R. Dandekar, "WiART-visualize and interact with wireless networks using augmented reality," in *Proceedings of the 22nd Annual International Conference on Mobile Computing and Networking*, 2016, pp. 511–512.
- [7] Q. Liao, I. Malanchini, V. Suryaprakash, and P. Baracca, "Method and apparatus for a radio communication network," May 2018, US Patent App. 15/799,542.
- [8] Q. Liao, S. Wesemann, I. Malanchini, and P. Baracca, "Haptic augmented reality assisted self-service for wireless networks," Sept. 2019, US Patent App. 16/347,029.
- [9] Q. Liao, "SLAMORE: SLAM with object recognition for 3D radio environment reconstruction," in *IEEE ICC*, 2020, pp. 1–7.
- [10] T. Hu and Q. Liao, "Real-time camera localization with deep learning and sensor fusion," in *IEEE ICC*, 2021, pp. 1–7.
- [11] C. Campos, R. Elvira, J. J. G. Rodríguez, J. M. Montiel, and J. D. Tardós, "ORB-SLAM3: An accurate open-source library for visual, visual-inertial, and multimap slam," *IEEE Transactions on Robotics*, vol. 37, no. 6, pp. 1874–1890, 2021.
- [12] M. Berger, A. Tagliasacchi, L. M. Seversky, P. Alliez, G. Guennebaud, J. A. Levine, A. Sharf, and C. T. Silva, "A survey of surface reconstruction from point clouds," in *Computer Graphics Forum*, vol. 36, no. 1. Wiley Online Library, 2017, pp. 301–329.
- [13] Z. Yun and M. F. Iskander, "Ray tracing for radio propagation modeling: Principles and applications," *IEEE Access*, vol. 3, pp. 1089–1100, 2015.
- [14] R. Hoppe, G. Wölfle, and U. Jakobus, "Wave propagation and radio network planning software WinProp added to the electromagnetic solver package FEKO," in *IEEE ACES*, 2017, pp. 1–2.
- [15] R. Valenzuela, "A ray tracing approach to predicting indoor wireless transmission," in *IEEE 43rd Vehicular Technology Conference*, 1993, pp. 214–218.
- [16] S. Kasdorf, B. Troksa, C. Key, J. Harmon, and B. M. Notaroš, "Advancing accuracy of shooting and bouncing rays method for ray-tracing propagation modeling based on novel approaches to ray cone angle calculation," *IEEE Transactions on Antennas and Propagation*, vol. 69, no. 8, pp. 4808–4815, 2021.
- [17] M. Sandler, A. Howard, M. Zhu, A. Zhmoginov, and L.-C. Chen, "MobileNetV2: Inverted residuals and linear bottlenecks," in *IEEE CVPR*, 2018, pp. 4510–4520.